Engineering 24 (2023) 264–275

Contents lists available at ScienceDirect

Engineering

journal homepage: www.elsevier.com/locate/eng

Research
Environmental Engineering—Article

Long-Term Cultivation and Meta-Omics Reveal Methylotrophic Methanogenesis in Hydrocarbon-Impacted Habitats

Yi-Fan Liu [a,d,e,#], Jing Chen [a,e,#], Zhong-Lin Liu [a], Zhao-Wei Hou [b], Bo Liang [a,e], Li-Ying Wang [a,e], Lei Zhou [a,e], Li-Bin Shou [a,e], Dan-Dan Lin [a,e], Shi-Zhong Yang [a,e], Jin-Feng Liu [a,e], Xiao-Lin Wu [b,*], Ji-Dong Gu [c], Bo-Zhong Mu [a,e,*]

[a] State Key Laboratory of Bioreactor Engineering and School of Chemistry and Molecular Engineering, East China University of Science and Technology, Shanghai 200237, China
[b] Exploration and Development Research Institute of Daqing Oilfield Company Limited, PetroChina, Daqing 163712, China
[c] Environmental Engineering and Engineering Group, Guangdong Technion Israel Institute of Technology, Shantou 515063, China
[d] Shanghai Institute of Pollution Control and Ecological Security, Shanghai 200092, China
[e] Engineering Research Center of Microbial Enhanced Oil Recovery (MEOR), East China University of Science and Technology, Shanghai 200237, China

ARTICLE INFO

Article history:
Received 1 April 2021
Revised 14 July 2021
Accepted 4 August 2021
Available online 10 January 2022

Keywords:
Methanogenic hydrocarbon degradation
Oily sludge
Bioremediation
Alkanes

ABSTRACT

The microbial conversion of alkanes to methane in hydrocarbon-contaminated environments is an intrinsic bioremediation strategy under anoxic conditions. However, the mechanism of microbial methanogenic alkane degradation is currently unclear. Under ten years of continuous efforts, we obtained a methanogenic *n*-alkane-degrading (C_{15}–C_{20}) enrichment culture that exhibited sustained improvements in the kinetic properties of methane production. The integrated metagenomic and metatranscriptomic analyses revealed that *n*-alkanes were mainly attacked by members of Desulfosarcinaceae, Firmicutes, and Synergistetes using the fumarate addition strategy, and were then further degraded in a common effort by *Tepidiphilus* members. Meanwhile, the abundant members of Anaerolineaceae were mainly responsible for cell debris recycling. However, according to the metatranscriptomic analyses, methane was predicted to be produced mainly via H_2-dependent methylotrophic methanogenesis, primarily from necromass-derived trimethylamine mediated by Methanomethyliaceae within the candidate phylum Verstraetearchaeota. These findings reveal that H_2-dependent methylotrophic methanogens, as well as methylotrophic methanogens, may play important ecological roles in the carbon cycle of hydrocarbon enriched subsurface ecosystems.

1. Introduction

The worldwide use and distribution of crude oil and its derivatives has led to hydrocarbon contamination in various environments [1]. Alkanes, which comprise the major fraction of crude oils, are commonly found in hydrocarbon-contaminated habitats [2]. Environmental contamination with high organic loads usually results in the development of anoxic conditions, under which alkanes can be naturally converted to methane via microorganisms [3] after nitrate, iron(III), and sulfate are depleted as electron acceptors [4]. Despite having been studied for two decades, beginning with the first definitive enrichment culture that produced methane from *n*-hexadecane [5], the underlying mechanism of methanogenic alkane degradation has not yet been fully resolved.

Several studies have shown that methanogenic alkane degradation requires the concerted efforts of metabolically different types of microorganisms [6], including an initial attack on the inert C–H bond of alkane compounds by syntrophic/fermentative bacteria, subsequent conversion to methanogenic substrates (such as formate, H_2, and acetate), and methanogenic archaea that consume these substrates to a very low level to keep the overall biodegradation process thermodynamically favorable [7].

Among the bacterial members, Deltaproteobacteria, especially the genus *Smithella*, are continuously detected and often dominant in low- to high-temperature methanogenic alkane degradation enrichment cultures from different sources [5,8–12]. Increasing studies based on single-cell and metagenomic sequencing have

* Corresponding authors.
E-mail addresses: wuxldq@petrochina.com.cn (X.-L. Wu), bzmu@ecust.edu.cn (B.-Z. Mu).
# These authors contributed equally to this work.

https://doi.org/10.1016/j.eng.2021.08.027

revealed that *Smithella*-like genomes contain genes encoding canonical alkylsuccinate synthase (ASS) [9,10], which catalyzes alkane activation via the addition of fumarate. Meanwhile, studies based on metatranscriptomic and reverse transcription-polymerase chain reaction (PCR) analyses have definitively demonstrated that ASS gene (*assA*) affiliated with *Smithella* are expressed during methanogenic alkane degradation [9,10]. Therefore, it has been proposed that members of *Smithella* are major "alkane breakers," via fumarate addition in methanogenic alkane-degrading cultures [11,12].

Archaeal communities in methanogenic alkane-degrading cultures, however, are often made up of hydrogenotrophic (e.g., *Methanocalculus* and *Methanoculleus*) and acetoclastic methanogens (e.g., *Methanosaeta*) [6,10,13]. In a study considering a methanogenic hexadecane-degrading enrichment culture [5], more than 2/3 of the methane was predicted to be produced from acetate, and thermodynamic calculations indicated that hexadecane conversion to methane is driven primarily via acetoclastic methanogenesis [14]. Meanwhile, by modeling isotopic signatures for gaseous CO_2 and methane collected from heavily degraded oils in the mesothermic Peace River Oil Sands, it was suggested that hydrogenotrophic methanogenesis likely predominates in subsurface degraded oil reservoirs where the most easily degradable compounds are straight-chain *n*-alkanes [15]. A similar result was obtained from a DNA-stable isotope probing (SIP)-based study of a methanogenic ^{13}C-hexadecane degrading consortium, where hydrogenotrophic methanogens were found to be dominant in the heavy DNA fractions [16]. Another radiotracer experiment using ^{14}C-labeled bicarbonate and acetate as substrates revealed that the rates of hydrogenotrophic methanogenesis were 42–68 times greater than those of acetoclastic methanogenesis. Furthermore, a metatranscriptomic analysis of alkane-degrading enrichment consortia [9,17] and production water samples [18] collected from oil reservoirs suggested that hydrogenotrophic and acetoclastic methanogenesis are the main pathways for converting alkane-derived substrates into methane. These results collectively support the exclusive role of hydrogenotrophic CO_2-reducing and acetoclastic methanogenesis in the decomposition of oil alkanes in anoxic hydrocarbon-associated environments [8]. However, alternative methanogenesis pathways, such as methylotrophic methanogenesis and H_2-dependent methylotrophic methanogenesis, are often overlooked, despite the fact that methanogens (such as the *Methanohalophilus*, *Methanolobulus*, and *Methanosarcina* species) that can use methyl compounds to produce methane were commonly detected in hydrocarbon-associated environments [19,20]. Although methane generation from methylated C_1 compounds is possible, it is difficult to envision those methylated compounds can be produced during the degradation of alkanes or other hydrocarbon molecules [21].

In a previous study, Wang et al. [22] obtained methanogenic enrichment cultures from oily sludge (OS), and the following transfer was amended with *n*-alkanes (C_{15}–C_{20}) as the sole carbon and energy source. Subsequent transfer by Liang et al. [23] into fresh medium resulted in a methanogenic alkane-degrading enrichment culture after more than 1300 days. A phylogenetic analysis based on the 16S ribosomal RNA (rRNA) gene and methyl coenzyme M reductase gene (*mcrA*) amplicon libraries showed that members of Anaerolineaceae and *Methanosaeta* dominated the bacterial and archaeal communities, respectively [19]. Hence, Anaerolineaceae was proposed to play an important role in fermentation and alkane oxidation, and *Methanosaeta* was mainly responsible for methane production via the acetoclastic pathway [19]. However, because of a lack of cultured representatives and genomic information, the exact functions of Anaerolineaceae and other organisms in the culture remain largely unknown.

To study the mechanism of methanogenic alkane degradation and resolve the roles of microorganisms in the community, we conducted a third transfer from a long-term *n*-alkane-degrading (C_{15}–C_{20}) enrichment culture. The cells were harvested at the late exponential phase of methane production and investigated for microbial metabolic potential and transcriptional activity using an integrated metagenomic and metatranscriptomic method.

2. Material and methods

2.1. Establishing enrichment cultures

The initial enrichment culture was established in a previous study using OS collected from the Shanghai Oil Refinery (China) [22]. Enrichment cultures in this study (the third transfer) were established by transferring approximately 10 mL (20% v/v) of the second transfer culture with a mixture of *n*-alkanes (C_{15}–C_{20}) incubated long-term as previously described [23,24] in a 120 mL autoclaved serum bottles that included 40 mL sterile basal medium (0.20 g·L^{-1} NaCl, 1.20 g·L^{-1} $MgCl_2·6H_2O$, 0.10 g·L^{-1} $CaCl_2·2H_2O$, 0.25 g·L^{-1} NH_4Cl, 0.20 g·L^{-1} KH_2PO_4, 1.30 g·L^{-1} KCl, 2.50 g·L^{-1} $NaHCO_3$, and 0.0001 g·L^{-1} rezasurin), and 1.0 mL·L^{-1} of vitamin stock solution and trace element stock solution [20]. The basal medium was reduced by adding 0.50 g·L^{-1} $Na_2S·9H_2O$ to the medium and adjusted to a final pH of 7.2, after which it was sealed with butyl rubber stoppers and aluminum crimps (Bellco Glass, Inc., USA). Each sample (three replicates) was supplemented with 15 μmol of each *n*-alkane (C_{15}, C_{16}, C_{17}, C_{18}, C_{19}, and C_{20}) (≥ 99%; Sigma-Aldrich, USA) as described previously [23], and incubated at 37 °C in the dark for more than three years.

2.2. Methane detection

Methane accumulation was periodically monitored via gas chromatography (GC; Agilent 6890; Agilent Technologies, Inc., USA) using the standard calibration curve for methane (R^2 = 0.994, n = 6). Specifically, 200 mL of headspace gas was injected into the GC using a sterile micro-syringe. The procedures was as follows: the initial column temperature was set to 60 °C for 12 min, increased to 200 °C at a rate of 15 °C·min^{-1}, and then maintained at 200 °C for 24 min. The temperatures of the injector, flame ionization detector, and thermal conductivity detector were maintained at 200 °C.

2.3. Kinetic model of methane production

The modified Gompertz model (Eq. (1)) is one of the most suitable models for fitting the growth of microorganisms [25]. Therefore, the modified Gompertz model was used to process the experimental data for the lag phase, maximum methane production rate, and methane yield potential under the assumption that the rate of biogas production is proportional to the microbial activity in the bioreactor. The modified Gompertz model is as follows:

$$Y = A_m \times \left\{ -\exp\left[\frac{V_m \times e}{A} (t_{lag} - t) + 1 \right] \right\} \quad (1)$$

where Y represents the cumulative biogas production (μmol) in the bioreactor at an incubation time, t (d), A_m is the maximum biogas yield potential (μmol), V_m is the maximum biogas production rate (μmol·d^{-1}), t_{lag} is the lag phase (d), and e is the natural constant (2.7183). Note that the A_m, V_m, and t_{lag} constants were estimated based on the triplicate datasets using Origin8.0 (Originlab Corporation, USA).

2.4. PCR amplification

The primers for the canonical *assA* genes have been described previously [19]. The PCR conditions were as follows: 95 °C for 5 min, followed by 38 cycles of 95 °C for 30 s, 52–58 °C for 45 s, 72 °C for 60–90 s, and a final elongation step at 72 °C for 10 min. The annealing temperature and extension time for each primer were modified according to the manufacturer's instructions (Appendix A Table S1).

2.5. Chemical analysis

Residual *n*-alkanes and intermediate fatty acids in the enrichment culture were detected at the end of incubation using gas chromatography–mass spectrograph (GC–MS; Agilent 6890 GC) fitted with an HP-5MS capillary column (30 m × 0.25 mm × 0.25 μm), in which the 5975 MS was run in the full-scan mode (Agilent Technologies, Inc.) [19]. To extract the residual alkanes, 50.0 μL of cetyl chloride was added to the serum bottles as a surrogate standard, after which the entire serum bottle was extracted with *n*-hexane and subsequently dried over anhydrous Na_2SO_4. The pooled organic layer was then transferred to a new vial and concentrated under a stream of N_2. The extracts were injected into the GC–MS with the following program settings: initial oven temperature of 120 °C for 3 min, and then increased to 260 °C at a rate of 8 °C·min^{-1}, at which the temperature was maintained for 10 min. The GC peak area of the surrogate standard (cetyl chloride) and alkanes ranging from C_{15} to C_{20} were integrated to obtain the *n*-alkane-to-standard ratio. Finally, the quantity of each *n*-alkane was determined based on the peak area ratio.

Long-chain fatty acids (LCFAs) and volatile fatty acids (VFAs) were detected by taking 5 mL of culture aliquot from the triplicate samples, adding ammonia water to raise the pH to more than 12, and drying in an oven at 110 °C. This was followed by esterification at 90 °C for 60 min by adding 0.5 mL 10% butanol/sulfate solution. Then, the esterified derivatives were extracted with 0.5 mL *n*-hexane and 0.5 mL *n*-dodecane. After, the extracts were injected into the GC–MS for detection. For the LCFA analysis, the oven temperature was maintained at 120 °C for 3 min and increased at a rate of 8 °C·min^{-1} to 260 °C, where it was maintained for 10 min. Conversely, for the VFA analysis, the oven temperature was maintained at 60 °C for 1 min and then increased to 130 °C at a rate of 15 °C·min^{-1}.

The theoretical methane yield was calculated using the Buswell equation [25], which represents the complete oxidation of alkanes to methane and CO_2 (Eq. (2)). The equation was modified as previously described [23] (Eq. (3)) by considering the intermediate or dead-end metabolites detected from the incomplete oxidation of alkanes. This calculation was further modified by subtracting the amount of carbon in the intermediate metabolites (including LCFAs and VFAs) from the total consumed alkanes.

$$C_nH_{2n+2} + (n/2 - 0.5)H_2O \rightarrow (0.25n - 0.25)CO_2 + (0.75n - 0.25)CH_4 \quad (2)$$

$$\text{Carbon}'_{\text{consumed alkanes}} = \text{Carbon}_{\text{consumed alkanes}} - \sum \text{Carbon}_{\text{intermediates}} \quad (3)$$

To measure the cations and anions in the culture, 2 mL of medium from the triplicate cultures was extracted and centrifuged before the supernatant was further filtered. The anion concentrations of Cl^-, NO_3^-, PO_4^{3-}, CO_3^{2-}, SO_4^{2-}, and $S_2O_3^{2-}$ were measured using an ion chromatography model ICS-1100 (Dionex, USA) equipped with an IonPac AS11-HC (Thermo Scientific, USA) column (temperature: 30 °C; eluent: KOH elution; detector: conductivity detector and ampere detector; suppressor: anion suppressor SHY-A-6; Shine Technology, China). Meanwhile, the cation concentrations of K^+, Mg^{2+}, Ca^{2+}, methylamine, dimethylamine, and trimethylamine were measured using ion chromatography model IC25A (Dionex) equipped with an IonPac CS17 (Thermo Scientific) column (temperature: 35 °C; eluent: 20 mmol·L^{-1} methylsulfonic acid isocratic elution; detector: conductivity detector; suppressor: cation suppressor, CERS-500, Thermo Scientific). For Na^+ and ammonia detection, an ion chromatography model CIC-D120 (Shine Technology) equipped with an SH-CC-3 (Shine Technology) column was used.

2.6. DNA/RNA extraction and 16S rRNA high-throughput sequencing

After more than 1400 days of anaerobic incubation, the total DNA and RNA were extracted from the pellets of one of the biological triplicates using a PowerSoil DNA Isolation Kit (MO BIO, USA) and a PowerMicrobiome™ RNA Isolation Kit (MO BIO), respectively. To enrich the messenger RNA (mRNA), rRNA was depleted from the total RNA using a Ribo-Zero rRNA Removal Kit (Bacteria) (Illumina®, USA) according to the manufacturer's instructions. The complementary DNA (cDNA) was synthesized as previously described [9]. The bacterial and archaeal 16S rRNA genes were PCR-amplified from metagenomic DNA using primer sets 515F/907R [26] and 344F/915R [27], respectively. All 16S rRNA gene amplicon libraries were sequenced on an Illumina Hiseq 2500 platform, generating 250 base pairs (bp) paired-end reads. Quality filtering, paired-end read merging, adapter removal, and primer trimming were performed as described previously [11]. The high-quality sequences obtained using the Illumina Miseq platform (Majorbio, China) were clustered into operational taxonomic units at a 97% similarity level based on the SILVA database (release 123; Germany) [28].

2.7. Metagenomic and metatranscriptomic sequencing

Metagenomic sequencing and metatranscriptomic libraries were generated using the NEB Next® Ultra™ DNA Library Prep Kit for Illumina® (New England Biolabs, USA), in accordance with the manufacturer's recommendations, to which the index codes were added. The library quality was assessed using a Qubit 3.0 Fluorometer (Life Technologies, USA) and Agilent Technologies, Inc. 4200 (Agilent Technologies, Inc.) system. Finally, the library was sequenced on an Illumina Hiseq X-ten platform, generating a total of 150 bp paired-end reads.

2.8. Metagenomic assembly and binning

Raw reads were quality-filtered, and adapters were removed using Trim_galore[†] under the default settings. Filtered reads of the metagenome dataset were assembled using metaSPAdes v3.7.0 with "*k*-mer = 127" [29], and all contigs shorter than 500 bp were removed. Read mapping was performed using Bowtie 2 [30], after which the mapped reads were filtered by removing the reads with a mapping quality of less than 3 [31] in order to remove ambiguously mapped reads. The resulting sequence alignment/map (SAM) file was sorted and converted into a binary alignment/map (BAM) file using SAMtools v1.6 [32]. Scaffolds were binned into population genomes using three different tools based on different clustering algorithms and features: ① MaxBin 2 v2.2.3 [33], which is based on an expectation–maximization algorithm, uses tetranucleotides, differential coverage, and marker genes, and was used with marker gene sets of 107 and 40 for bacterial and archaeal lineages, respectively; ② MetaBAT2 v0.32.4 [34], which applies a *k*-medoid clustering on tetranucleotide

[†] http://www.bioinformatics.babraham.ac.uk/projects/trim_galore/.

frequencies and differential coverage, was used with its default settings; and ③ CONCOCT v0.4.0 [35] uses Gaussian mixture models and tetranucleotide frequencies with differential coverages. The resulting bins were supplied to the DAS Tool (v1.1.1) for consensus binning and de-replication, generating an optimized set of metagenome-assembled genomes (MAGs) [36]. The resulting MAGs were further refined by removing outlier scaffolds by setting the percentile of divergent guanine and cytosine, sequencing coverage, and tetranucleotide frequencies to 95 in RefineM v0.0.23 [37]. Subsequent manual checks were performed using Anvi'o v5 [38]. Briefly, the MAGs were split into major clusters based on their split coverage and guanine and cytosine content. These clusters were merged if the separated clusters were parallel in the same genome tree position.

2.9. Taxonomic and functional annotation

Genes from the entire assembly were labeled by Prodigal v2.6 [39] in "meta" mode. Then, the amino acid files were submitted to the GhostKOALA server [40] in the prokaryotic species database to assign the KEGG orthology (KO) numbers. Additionally, the carbohydrate-active genes were identified in the dbCAN web server [41] with cutoffs used in a previous study [42] (coverage > 0.40; *E*-value < 1×10^{-18}; identity > 30%). Genes involved in anaerobic hydrocarbon degradation were identified using Blastp via a comparison with a previously reported database [42] (coverage > 0.40 ; *E*-value < 1×10^{-20}; identity > 30%). Hydrogenases were first identified using the HMMER (v3) search function [43] (*E*-value < 1×10^{-20}) with custom HMM models (Appendix A File S1), and hits were further classified into different hydrogenase groups on the HydDB web server [44]. We also uploaded the nucleotide MAG sequences to the RAST server to confirm the gene annotations using subsystem technology [45]. Taxonomic assignments of the unbinned genes were performed using Kaiju [46] against the national center for biotechnology information (NCBI) *nr_euk* database (2018-7-20) in "Greedy" mode. Finally, the taxonomic classification of the MAGs was mainly based on GTDBtk (release 86) prediction[†], which uses recently described relative evolutionary distance metrics to predict the divergence of newly binned clades [47]. The classifications were further verified using a polygenetic analysis of the conserved protein sequences and 16S rRNA gene sequences.

2.10. Genome coverage and gene FPKM calculation

To estimate the genome sequencing coverage, we pooled the scaffold files of the final MAGs, the corresponding read mapping files generated from the metagenomic dataset, and the metatranscriptomic dataset into Anvi'o v5 [38] after filtering to remove reads with a mapping quality of less than 3, as previously described. The mean coverage for the inner quartiles (Q2 and Q3) for each MAG was estimated by summarizing the metagenome and metatranscriptome profiles. We used eXpress v1.5.1 [48] to calculate the fragments/kilobase of transcript per million fragments mapped (FPKM) of individual genes, in which the entire assembly was used as an input file. The FPKM values of the metagenome and metatranscriptome datasets (referred to as FPKM in this study) were individually calculated using sorted BAM files derived from the read mapping of the metagenome and metatranscriptome datasets, respectively.

2.11. Phylogenetic analysis

The small subunit rRNA genes in the MAGs were identified using checkM v1.0.16 [37] with the "ssu_finder" function, and sequences longer than 400 bp were used for the phylogenetic analysis. The selected sequences were aligned using MAFFT [49] with iterative refinement methods "G-INS-i," before they were manually refined (retained columns with < 10% gaps). To construct the genome tree, all reference genomes (listed in Appendix A Table S2) and MAGs were pooled into PhyloPhlAn v0.99, which extracted and aligned 400 conserved protein sequences [50]. The concatenated alignment file was then extracted for phylogenomic tree building. For both alignments, maximum likelihood trees were reconstructed using IQ-tree v1.6.7, under standard model selection with 1000 ultrafast bootstrap conditions. The trees were further decorated using Inkscape v0.92.3[‡] and visualized using iTOL [51].

2.12. Data availability

The raw sequence data used in this study were submitted to the NCBI database under BioProject PRJNA792315.

3. Results

3.1. Ten-year successive enrichment

In this study, we set up an enrichment culture with OS as the inoculum and an *n*-alkane mixture (C_{15}–C_{20}) as the sole carbon and energy source [19,22]. After ten years of cultivation and three consecutive transfers, the culture was found to improve the kinetic properties of methane production. This was concluded by considering the period of the lag phase, the maximum methane concentration, and the maximum methane production rate (Fig. 1 and Appendix A Fig. S1). In the third transfer, the culture produced a total of 352 μmol of methane 1413 days after a lag phase of 267.1 days (predicted by fitting the data into the modified Gompertz model [24,52]) (Fig. 1 and Fig. S1). After incubation, almost all *n*-alkanes were depleted (Appendix A Table S3), and putative degrading intermediate metabolites, including octadecanoate, hexadecanoate, tetradecanoate, dodecanoic, butyrate, propionate, acetate, and formate, were detected in the culture (Appendix A Table S4). The detected methane in the third transfer accounted for 63.4%–71.5% of the theoretical methane yield.

3.2. Microbial community succession

The biomass in the third transfer was harvested during the late-exponential methane production phase for nucleotide sequencing (Fig. 1). Based on the 16S rRNA gene survey results, the microbial communities varied greatly over the incubation period (Fig. 2). Compared with the second transfer, the four major bacterial lineage (Enterobacteriaceae, Unclassified_Cloacimonadales, Ignavibacteriaceae, and Leptospiraceae) concentrations decreased by more than 50% in the third transfer (Fig. 2). Subsequently, Hydrogenophilaceae, Anaerolineaceae, and Desulfosarcinaceae, which accounted for more than 80% of the bacterial community composition, became the dominant bacteria (Fig. 2). Lineages such as Syntrophaceae, Synergistaceae, Thermodesulfovibrionaceae, and Kosmotogaceae, which were found to be occasionally detected in OS samples, the initial culture, or the first transfer, existed at concentrations below the detection limit in the second transfer sample, but were detected in low abundance in the third transfer (Fig. 2). This variation might be because of the extremely low abundance of these minor members in the samples, which could be overlooked when applying low-throughput amplicon sequencing from clone libraries [19].

[†] https://github.com/Ecogenomics/GTDBTk.

[‡] https://inkscape.org/.

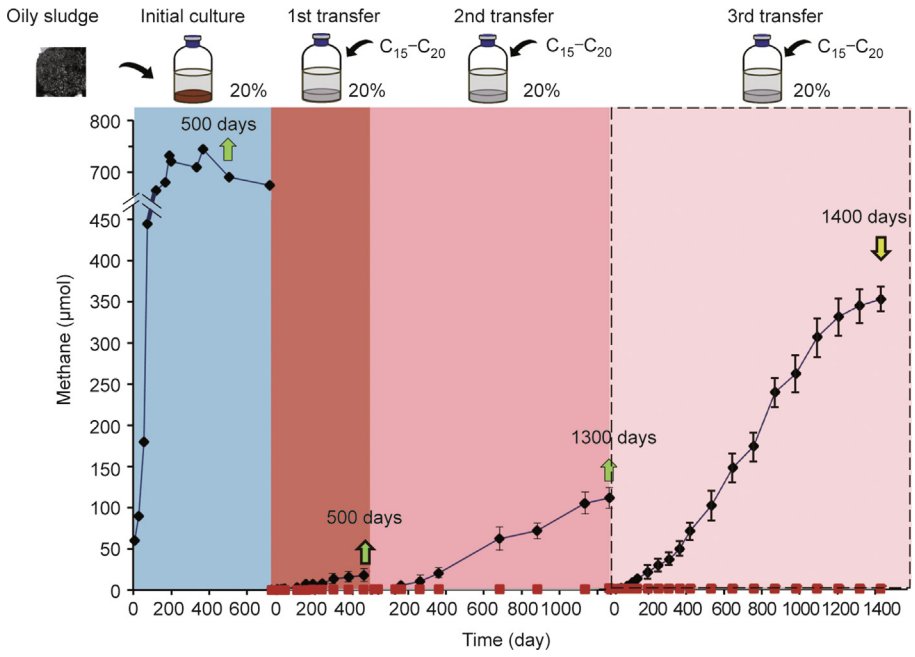

Fig. 1. Methane production values of the *n*-alkane-degrading enrichment cultures during three sequential transfers. Methane data from this study are marked with dotted borders. The curve with black diamonds represents the initial culture and subsequent enrichment cultures amended with the *n*-alkanes mixture (C_{15}–C_{20}) as the sole carbon and energy source (three replications), and the curve with red squares represents the *n*-alkanes-free control group (three replications). Error bars indicate the standard error of the mean of the biological triplicates. Each time point for transfer to the fresh medium is marked with a green arrow, and the time point for metagenomic and metatranscriptomic sequencing is marked with a yellow arrow.

The archaeal communities in all the samples from each stage were mainly composed of methanogenic lineages, including Methanomicrobiaceae, Methanosaetaceae, Methanosarcinaceae, Methanoregulaceae, and Methanocorpusculaceae. Compared with the second transfer, however, the dominant archaea members in the third transfer shifted from Methanosaetaceae (95.9% in the second transfer) to Methanosarcinaceae (51.2% in the third transfer). Methanomethyliaceae (22.4%), which is in the candidate phylum Verstraetearchaeota was detected for the first time in every stage of the third transfer. Note that the different PCR primers and sequencing techniques used for 16S rRNA gene amplicon sequencing could potentially bias the microbial composition [19,22].

The assembly and binning of metagenome data resulted in a total of 23 MAGs with > 50% completeness and < 10% contamination (estimated by CheckM [37]). Reconstructed MAGs comprised taxonomically diverse members from a total of 13 bacterial and 2 archaeal phyla (Fig. 3 [50] and Appendix A Table S5). Within the bacteria domain, members of the phylum Chloroflexi, especially the class Anaerolineae, were highly represented (6 of 23 MAGs with 7.8× to 198.5× mean sequencing coverage, as compared with the median coverage of 58.2× all MAGs, Appendix A Fig. S2). Within the archaea domain, two MAGs representing Methanosarcinaceae exhibited medium to high sequencing coverage (54.9× and 102.9× for Methanosarcinaceae archaeon bin5 and *Methanosarcina* sp. bin9, respectively; Fig. S2). We also found one Methanomethyliaceae-like MAG with a slightly lower sequencing coverage (46.7×) that represented the candidate phylum, Verstraetearchaeota. Overall, the pattern of MAG sequencing coverage was mostly in accordance with the microbial composition based on the 16S rRNA gene amplicon data. In total, 18 MAGs were classified into three classes, four orders, three families, and six genus level uncultured lineages that have not been described before (Fig. 3 and Table S5).

3.3. Anaerobic alkane degradation

To explore the metabolic potential of the third transfer, we analyzed the MAGs and the unbinned assembly fragments that could not be classified into any MAGs for specific functions (see Section 2). We used the FPKM values to demonstrate the relative abundances of the genes in the metagenome data, in which the FPKM values that ranked in the top 10% of all genes (i.e., FPKM > 13.0) were considered to be relatively high.

In this defined medium, the organic carbon source is derived from either inoculated *n*-alkanes (C_{15}–C_{20}) or detrital biomass [42]. To identify the potential for the microbial degradation of hydrocarbons, we searched for functional marker genes encoding enzymes that initiate anaerobic hydrocarbon biodegradation via the activation of C–H bonds [53]. The metagenomic results indicated a possible oxygen-independent C–H activation pathway, wherein there is *n*-alkane addition to fumarate (known as the fumarate addition pathway) [54] by glycyl-radical enzymes. Putative *assA*, which may mediate *n*-alkane addition to fumarate, were found in four MAGs (Desulfosarcinaceae bacterium bin16, Chloroflexi bacterium bin26, Phycisphaerae bacterium bin27, and *Spirochaetes* bacterium bin3), as well as several unbinned fragments representing Chloroflexi, Deltaproteobacteria, Alphaproteobacteria, Synergistetes, Firmicutes, Spirochaetes, Actinobacteria, and Candidatus (Ca.) Aminicenantes (Appendix A Fig. S3), with a high relative abundance (most FPKM values > 13.0; Fig. 4 and Appendix A Table S6). The *assA*-like sequences identified were phylogenetically distant from the canonical *Smithella*-like ASS [55] (amino acid identities < 45%), but formed a common clade with the putative ASS, which has been proposed to mediate alkane activation in anaerobic alkane degraders *Vallitalea guaymasensis* L81 [56], *Thermococcus sibiricus* MM 739 [57], and *Archaeoglobus fulgidus* VC-16 [18,58] (Fig. S3). Meanwhile, no *Smithella*-like MAGs or operational taxonomic units (OTUs) were generated from the metagenome or

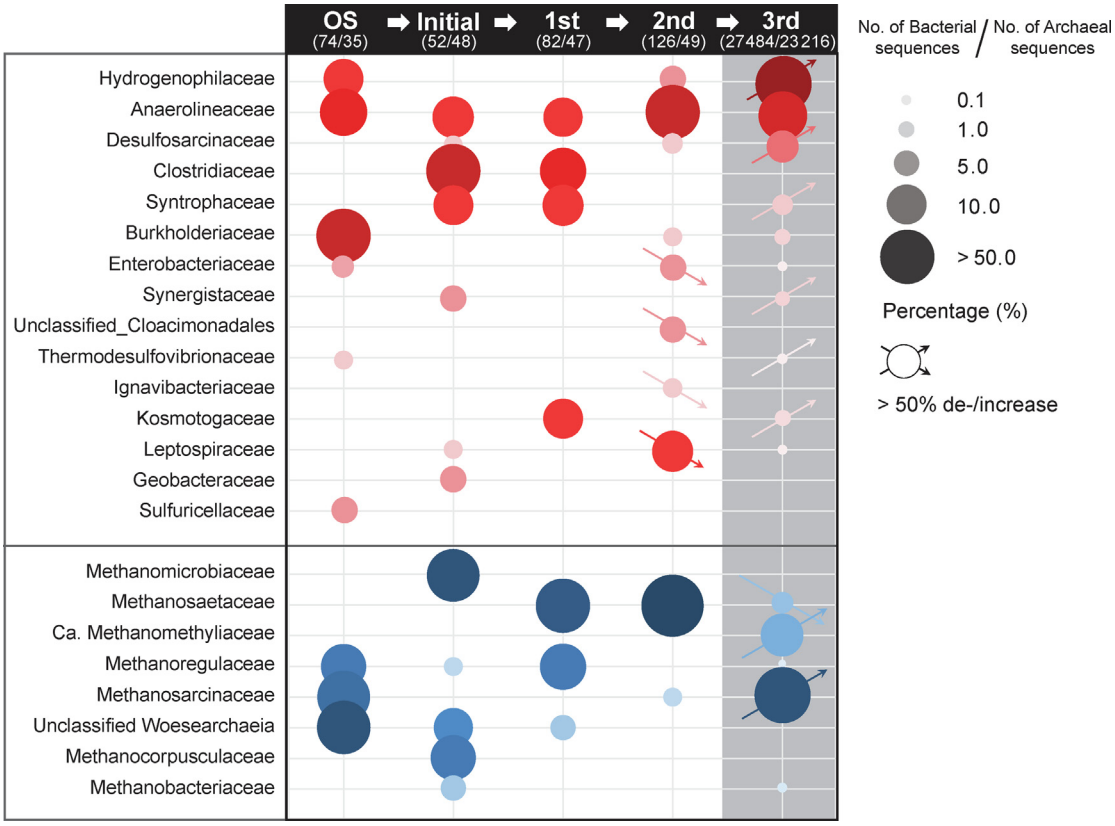

Fig. 2. Relative abundance of major microbial lineages (> 5% in at least one sample) at family level represented by 16S rRNA gene amplicon sequences detected in OS and enrichment cultures. 16S rRNA gene sequences from clone libraries of OS, initial culture (Initial), and two transfers were retrieved from previous studies [19,22], and the relative abundance based on the high-throughput 16S-tag sequencing of the third transfer is shaded in gray. The total sequences in the bacterial and archaeal libraries are also shown. Ca.: Candidatus; No.: numbers.

16S rRNA gene clone library. The lack of canonical *assA* was further verified via PCR amplification using previously designed canonical *assA*/adenosine triphosphate-binding cassette (*bssA*)-targeting primers (Table S6), as no amplicon sequences were retrieved from the samples.

Following the initial fumarate addition of alkanes, alkylsuccinates are converted to fatty acids through several steps, including acetyl-coenzyme A (CoA) activation, carbon skeleton rearrangement, and decarboxylation [59]. The genes involved in these steps, namely CoA-synthetase/ligase gene (*assK*), putative methylmalonyl-CoA mutase gene (*mcmLS*), and putative propionyl-CoA carboxylase gene (*pccAB*), were detected in several MAGs (Appendix A Table S7). However, no MAGs containing the putative *assA* gene contained the complete gene set required for alkylsuccinate metabolism, but some possessed a high degree of completeness (for example, the completeness of the Desulfosarcinaceae bacterium bin16 was 96.3%). Nevertheless, genes related to the pathway downstream of the *n*-alkane fumarate addition were found in several MAGs that did not have the *assA* (Table S7), suggesting an interplay between these MAGs and the *assA*-containing MAGs when degrading *n*-alkanes.

3.4. Necromass recycling and fermentation

In addition, necromass, which is mainly composed of complex carbohydrates, proteins, and lipids, could serve as a substrate for many community members in the third transfer [42]. On this basis, we searched for genes associated with peptide/amino acid degradation, complex carbohydrate degradation, and fatty acid degradation. Most of the MAGs (19 out of 23; Fig. 5 and Table S7) contained secreted carbohydrate-active enzymes and a near-complete Embden–Meyerhof pathway (glycolysis), suggesting the ability to break down complex carbohydrates from cell debris. Meanwhile, several genes encoding adenosine triphosphate-binding cassette (ABC)-type peptide transporters and amino acid transporters were observed in 11 MAGs (Fig. 5 and Table S7). Genes encoding peptidases, aminotransferases, 2-oxoacid-ferredoxin oxidoreductases, and aldehyde-ferredoxin oxidoreductases were also detected in these MAGs. Therefore, we inferred that these MAGs are capable of importing and degrading peptides step-wise into amino acids, then to 2-keto acids, and finally to acetyl-CoA [60]. Further, the genes required for fatty acid degradation (β-oxidation) were abundant in the metagenome data (Fig. 4), and a complete β-oxidation pathway was observed in seven bacterial MAGs (Fig. 5).

As no exogenous electron acceptors (e.g., oxygen, oxidized metal cations, oxidized sulfur compounds, or oxidized nitrogen compounds) were supplied to the enrichment culture, the heterotrophic microorganisms were usually disposed of catabolism-derived reducing equivalents by either producing H_2 or fermentation. Genes encoding H_2 evolving-only hydrogenases ([FeFe] group A/B and [NiFe] group 4a/b/d/g) were found in 17 MAGs, whereas hydrogenases for H_2 utilization were found in 13 MAGs (Fig. 5). Various MAGs and assembled fragments contained genes that indicated the capability for the fermentative production of lactate (6 MAGs) and ethanol (12 MAGs) (Figs. 4 and 5). Moreover, acetogenic CO_2 reduction via the Wood–Ljungdahl pathway could be an alternative pathway for the disposal of electrons derived from hydrocarbon/necromass oxidation [61,62]. Nearly all the bacterial MAGs contained orthologous genes that are responsible for acetate formation. However, complete gene sets for the Wood–Ljungdahl pathway were only found in four bacterial MAGs (Fig. 5), of which the Wood–Ljungdahl pathway found in the Methanosarcinaceae

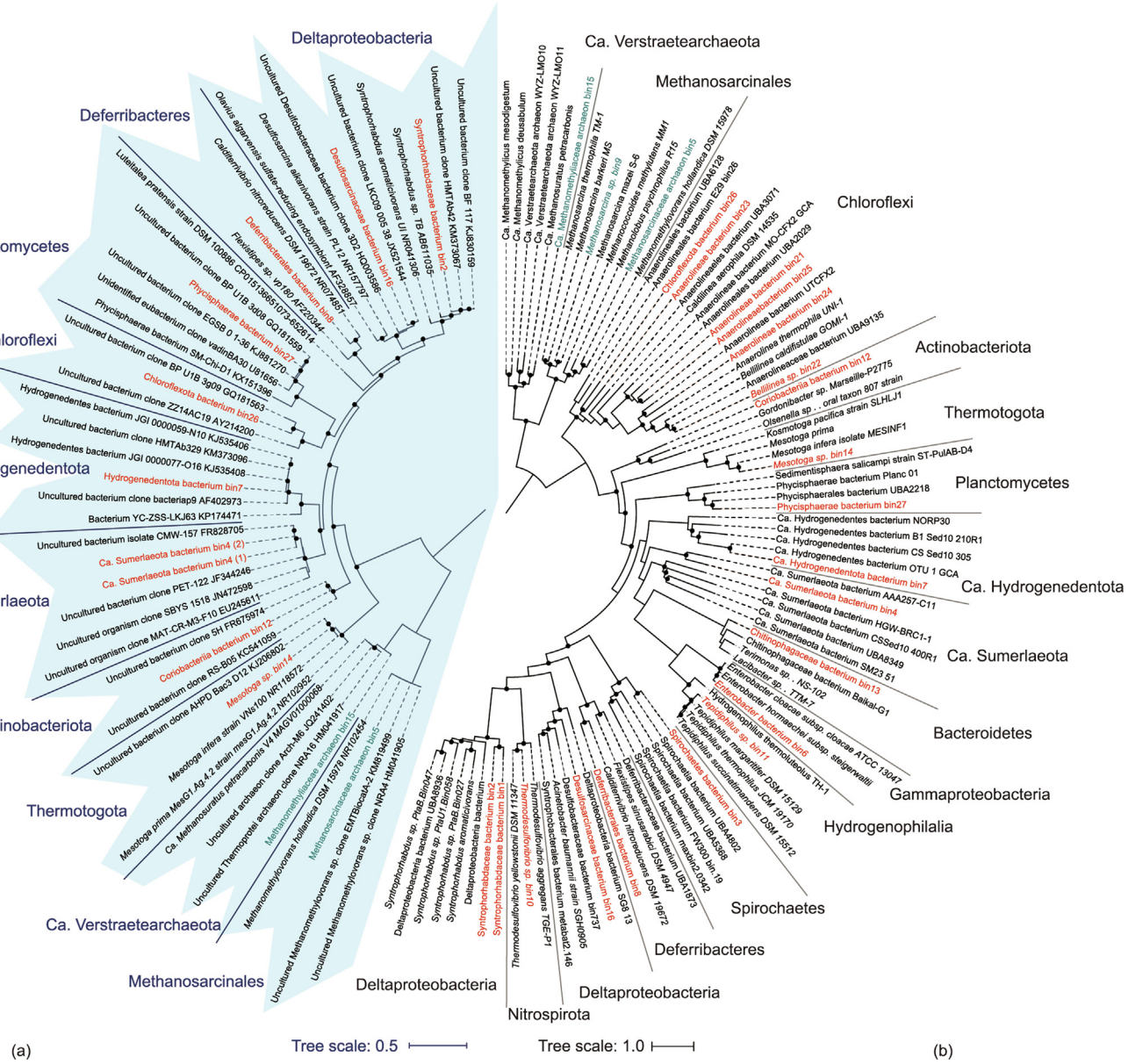

Fig. 3. Phylogenetic placement of reconstructed metagenome-assembled genomes. (a) Phylogenetic affiliation of the metagenome-assembled genomes (MAGs) and reference microorganisms based on their 16S rRNA genes, shaded in blue. (b) Phylogenomic affiliation of 23 MAGs based on 400 conserved protein sequences [50]. Both alignments are based on MAFFT and then filtered with columns containing > 90% gaps. The trees were built using IQ-Tree under the standard model selection with 1000 bootstrap replicates. Bootstrap values > 80% are indicated. The MAGs assembled in this study are marked in red for bacteria and green for archaea. Scale bars indicate the average number of substitutions/site.

MAGs was most likely associated with methanogenesis or biosynthesis [63].

3.5. Methanogenesis

To obtain the maximum free energy available from organic matter in the absence of external electron acceptors, microbial communities will continue their carbon turnover reactions until they reach the most thermodynamically stable states, that is, methane and CO_2 [64]. Genes specific for methanogenesis were only found in members of Methanosarcinales (Methanosarcinaceae archaeon bin5 and *Methanosarcina* sp. bin9) and Methanomethyliales (Methanomethyliaceae archaeon bin15) (Fig. 4). Methyl-coenzyme M reductase genes in these MAGs were clustered with MCR enzymes that catalyze methane metabolism, rather than MCR-like complexes associated with anaerobic methane/alkane oxidation (Appendix A Fig. S4) [65,66]. Therefore, a putative role for methane production was proposed for these organisms. As all these methanogenic signature genes had a high abundance (FPKM > 13.0) (Fig. 4), they had a high potential for methanogenesis in the sample. Furthermore, the complete gene sets for hydrogenotrophic, acetoclastic, and methylotrophic methanogenesis from methanol and tri/di/methylamine (T/D/MMA) were found in the MAGs of *Methanosarcina* sp. bin9 and Methanosarcinaceae archaeon bin5, indicating a versatile metabolic potential (Fig. 5). Conversely, the genome analysis revealed a strict H_2-dependent methylotrophic methanogenic lifestyle for Methanomethyliaceae archaeon bin15 (Fig. 5), which is consistent with the previous description of this lineage [67].

With respect to the ubiquitous distribution of methylotrophic methanogenic capability in all three archaeal MAGs, we searched for genes responsible for methyl compound generation. Marker genes for converting choline, trimethylamine *N*-oxide, betaine, and *L*-carnitine (*cut*, *tor*, *grd*, and *cnt*) to trimethylamine (TMA),

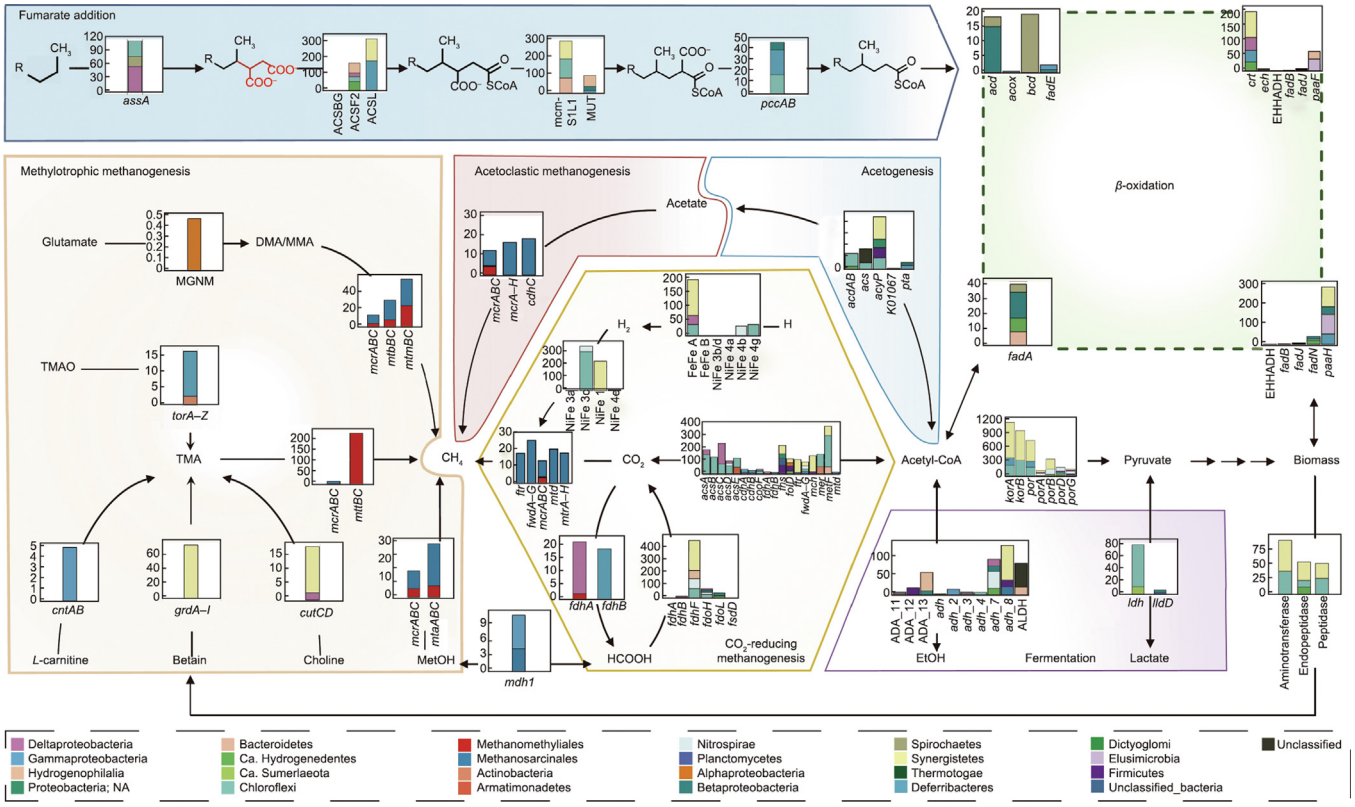

Fig. 4. Reconstruction of the potential carbon cycle in the third transfer. The FPKM values of the genes were summed according to their taxonomic assignment. Gene names: *fwd*, formylmethanofuran dehydrogenase gene; *ftr*, formylmethanofuran–tetrahydromethanopterin *N*-formyltransferase gene; *mer*, 5,10-methylenetetrahydromethanopterin reductase gene; *mtd*, methylenetetrahydromethanopterin dehydrogenase gene; *mch*, methenyltetrahydromethanopterin cyclohydrolase gene; *mcr*, methyl-coenzyme M reductase alpha subunit gene; *mtr*, N^5-methyltetrahydromethanopterin:coenzyme M methyltransferase; *acs*, acetyl-coenzyme A (CoA) synthetase (EC: 6.2.1.1) gene; *acd*, acetate-CoA ligase (adenosine diphosphate (ADP)-forming) gene; *cdh*, acetyl-CoA decarbonylase/synthase; *mta*, methanol-5-hydroxybenzimidazolylcobamide Co-methyltransferase gene; *mtm*, methylamine-corrinoid protein co-methyltransferase; *mtb*, dimethylamine-corrinoid protein Co-methyltransferase; *mtt*, trimethylamine-corrinoid protein co-methyltransferas gene; *acox*/*fadE*/*acd*/*bcd*, acyl–acyl carrier protein (ACP) dehydrogenase gene; *paaF*/*crt*/*fadJ*/*fadB*/*ech*, enoyl-CoA hydratase gene; *fadJ*/*fadB*/*fadN*/*ech*/*paaH*/*EHHADH*, 3-hydroxyacyl-CoA dehydrogenase gene; *fadA*, acetyl-CoA acyltransferase gene. TMA, trimethylamine; *cut*, choline trimethylamine-lyase gene; *tor*, trimethylamine-*N*-oxide reductase (cytochrome c) gene; *grd*, betaine reductase gene; *cnt*, carnitine monooxygenase subunit gene; MGNM, methylamine–glutamate *N*-methyltransferase gene; *mdh*, methanol dehydrogenase gene; *ALDH*, aldehyde dehydrogenase gene; CoA, coenzyme A; *por*, pyruvate ferredoxin oxidoreductase gene; *metF*, methylenetetrahydrofolate reductase gene; *mut*, methylmalonyl-CoA mutase gene; *acyP*, acylphosphatase gene; ADA, acetaldehyde dehydrogenase gene; *kor*, 2-oxoglutarate/2-oxoacid ferredoxin oxidoreductase gene; *ldh*, *L*-lactate dehydrogenase gene; *fol*, methenyltetrahydrofolate cyclohydrolase gene; *fhs*, formate-tetrahydrofolate ligase gene; *cooF*, anaerobic carbon-monoxide dehydrogenase iron sulfur subunit gene. For clarity, the Embden–Meyerhof pathway genes were omitted, and more details are listed in Table S6.

and genes for glutamate conversion (*mgnm*) and methanol generation (*mdh1*) were observed in the metagenome data at varying abundances (Fig. 4), implying that these substrates are readily available.

3.6. Metatranscriptomic sequencing coverages

Based on the metatranscriptomic sequencing coverage, several MAGs (10 out of 23) exhibited zero transcriptional activity at the time of sampling (Fig. S2). Meanwhile, all the MAGs with metagenomic sequencing coverage above the median had transcripts, with the exceptions of *Methanosarcina* sp. bin9 and Syntrophorhabdaceae bacterium bin2. Specifically, *Tepidiphilus* sp. bin11 had the highest mean coverage (43.2×), followed by *Mesotoga* sp. bin14 (8.8×), Methanomethyliaceae archaeon bin15 (8.4×), Anaerolineaceae bacterium bin23 (7.2×), Anaerolineaceae bacterium bin21 (5.5×), Desulfosarcinaceae bacterium bin16 (4.8×), Ca. Hydrogenedentota bacterium bin7 (4.1×), *Bellilinea* sp. bin22 (3.4×), *Enterobacter* bacterium bin6 (2.8×), *Thermodesulfovibrio* sp. bin10 (2.6×), Coriobacteriia bacterium bin12 (1.2×), Deferribacterales bacterium bin8 (0.6×), and Ca. Sumerlaeota bacterium bin4 (0.6×) (Fig. S2).

3.7. Gene transcriptomic pattern

To analyze the specific functional activity in the metatranscriptome of the third transfer, the gene-specific transcriptional levels were calculated using the FPKM values obtained from the metatranscriptome data. As less than 5% of genes had transcripts, we defined the FPKM values higher than the median value of all transcribed genes (i.e., FPKM > 10.2) as relatively high.

Despite having been detected in several MAGs and unbinned fragments, only the *assA*-like genes in the Desulfosarcinaceae bacterium bin16 (FPKM = 38.0) and several fragments classified within the phyla Synergistetes and Firmicutes (FPKM = 3.3 and 8.1, respectively) were transcribed at the sampling time (Fig. 5 and Table S8 in Appendix A), which suggests that the members of Deltaproteobacteria (Desulfosarcinaceae bacterium bin16), Synergistetes, and Firmicutes are responsible for *n*-alkane activation in the culture. In addition to *assA*, the *assK* gene in Desulfosarcinaceae bacterium bin16 also had high-level transcripts (FPKM = 28.1). Further, the genes associated with pathways downstream of *n*-alkane fumarate addition in the *Tepidiphilus* sp. bin11 were all highly transcribed.

Regarding necromass recycling, the genes for peptide transport and degradation were transcribed in *Tepidiphilus* sp. bin11,

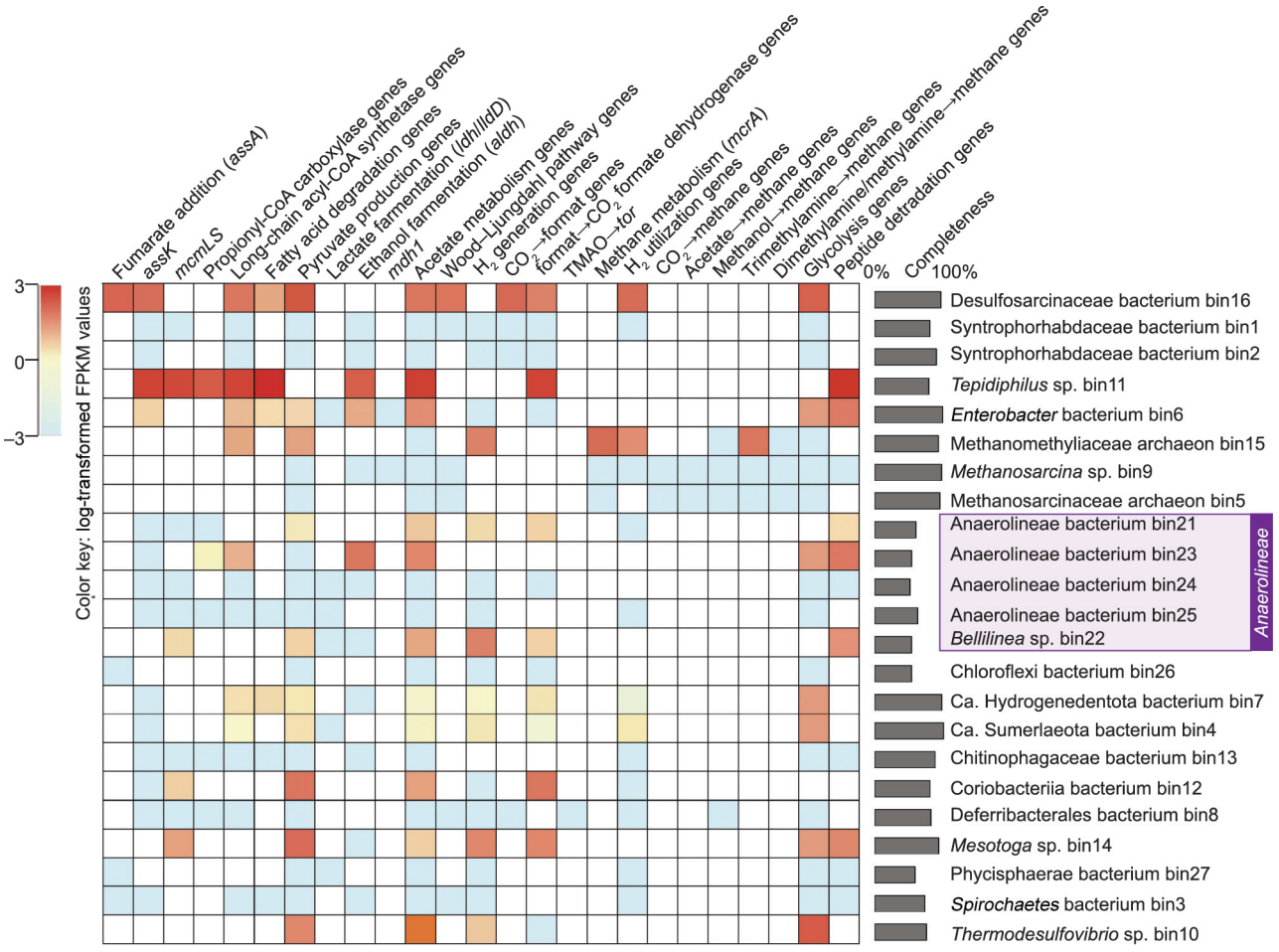

Fig. 5. Heatmap showing the transcription level of functional genes or pathways present in each MAG. MAGs with specific functional genes or pathways present are marked with color, and the transcriptional levels are expressed as the log-transformed FPKM (fragments/kilobase of transcript per million fragments mapped) values of the functional genes or the average value of all the detected genes in the pathways. Pathways are indicated as being present if ≥ 75% of the genes exist in the genome. TMAO: trimethylamine *N*-oxide.

Enterobacter bacterium bin6, Anaerolineaceae bacterium bin21 and bin23, *Bellilinea* sp. bin22, and *Mesotoga* sp. bin14 (Fig. 5). Meanwhile, the genes for intracellular and extracellular carbohydrate-active enzymes, as well as those involved in the Embden–Meyerhof pathway (glycolysis), were transcribed in Desulfosarcinaceae bacterium bin16, *Enterobacter* bacterium bin6, Anaerolineaceae bacterium bin23, Ca. Hydrogenedentota bacterium bin7, Ca. Sumerlaeota bacterium bin4, *Thermodesulfovibrio* sp. bin10, and *Mesotoga* sp. bin14 (Fig. 5). The transcriptional activity of fatty acid degradation was found in four MAGs: Desulfosarcinaceae bacterium bin16, *Tepidiphilus* sp. bin11, Ca. Hydrogenedentota bacterium bin7, and *Enterobacter* bacterium bin6 (Fig. 5).

Moreover, the genes for methanogenesis in *Methanosarcina* sp. bin9 and Methanosarcinaceae archaeon bin5 were both below the detection limit (Fig. S2), indicating a dormant state. Conversely, the genes related to methanogenesis, as well as the trimethylamine methyltransferase gene in Methanomethyliaceae archaeon bin15, were found to be highly transcribed (e.g., the FPKM values of *mcrA* and *mttB* were 20.3 and 13.7, respectively) with the transcripts of the H_2-utilizing gene. This suggests the H_2-dependent methylotrophic methanogenic activity of this organism. Regarding TMA production, the *cut* and *grd* genes encoded in unbinned fragments exhibited transcriptional activity (FPKM values of 3.2 and 14.9, respectively), whereas the genes generating other methyl compounds (methyl-/dimethyl-amine (M/DMA) and methanol) were inactive in the transcriptome.

4. Discussion

The succession of microbial communities during long-term incubation is considered to be the result of adapting to the cultivation environment. Thus, the change in microbial communities likely contributes to sustained improvements in the kinetic properties of methane production in the enrichment cultures. The dominant lineages in this culture were primary lineages that have been consistently detected in hydrocarbon-polluted environments, such as petroleum-contaminated soils [68], hydrocarbon-contaminated aquifers [1], and oil fields [69], thereby supporting the theory of the *in situ* microbial conversion of hydrocarbons to methane as a bioremediation strategy in hydrocarbon-polluted environments. However, exogenous nutrient supply (such as phosphate) may be required to establish an active methanogenic alkane-degrading microbial community, as hydrocarbon-polluted environments are usually limited to specific nutrients [70].

In this study, the metagenomic analysis revealed that the third transfer contained a wide range of uncultured lineages not observed in other habitats, which warrants an investigation into their metabolic potential. As revealed by the integrated metagenomic and metatranscriptomic analyses, the major organic carbon and energy sources in the cultures, *n*-alkanes, were utilized by anaerobic microorganisms via the fumarate addition pathway, wherein they were mediated by members of Deltaproteobacteria, Firmicutes, and Synergistetes at the time of sampling.

Furthermore, the pathway reconstruction from 23 MAGs recovered from the metagenome indicated incomplete fumarate addition in Desulfosarcinaceae bacterium bin16. The metatranscriptomic analysis suggested that *n*-alkane degradation via fumarate addition could be a joint achievement of Desulfosarcinaceae bacterium bin16 and *Tepidiphilus* sp. bin11. This expands the current understanding of *Smithella*, which is considered to be the major alkane breaker in many other low- to high-temperature alkane-degrading enrichment cultures [9,11,12,71,72]. In addition to *n*-alkanes, the microorganisms in the third transfer actively recycled cell debris, peptides/amino acids, carbohydrates, and fatty acids. We also propose that fermentation (ethanol) and acetogenic and syntrophic interactions (H_2) were major electron sinks for heterotrophic microorganisms, thereby driving microbial interactions. To date, microorganisms affiliated with Anaerolineaceae have been consistently detected in methanogenic cultures [10,71–73], and in a previous study, they were found to be the dominant bacteria in the second transfer [19]. However, the functional roles of these organisms in the *n*-alkane methanogenic are largely unknown due to the lack of genomic representatives [19,74]. In this study, we demonstrated that members of Anaerolineaceae in the third transfer were mainly responsible for the recycling of necromass. Consistent with this finding, a previous study examined an independent enrichment culture amended with ^{13}C-labeled hexadecane that used the same inoculum employed in this study and revealed that *Anaerolinea* and *Tepidiphilus* phylotypes have significantly higher relative abundances in the heavy fractions of DNA, as compared with the light fractions [75]. This result indicates the active involvement of *Tepidiphilus* in the transformation and biodegradation of alkanes and suggests the cross-labeling of *Anaerolinea* by incorporating ^{13}C from necromass [76] when considering the long-term incubation (920 days) [75].

In previous studies, hydrogenotrophic and acetoclastic methanogenesis have been considered to be the major processes downstream methanogenic hydrocarbon degradation [5,6,20,77]. However, in this study, metatranscriptomic analysis demonstrated the exclusive transcriptional activity of methanogenesis from methyl compounds. It has been proven that methanogenesis from methyl compounds is common where these compounds are abundant, such as marine sediments [78,79]. In this study, the methyl compounds derived from the necromass were readily available substrates for methanogenesis. Note that the Methanosarcinales MAGs constructed in this study have the metabolic potential to utilize hydrogen and methyl compounds for methane production (Fig. 4), but they were underrepresented in the metatranscriptome. This might be partially explained by the fact that methanogens without cytochromes (such as Methanomethyliaceae) usually outcompete methanogens with cytochromes (species within Methanosarcinales) for H_2 because they have a lower H_2 threshold concentration [63]. However, the exact relationship between the members of Methanomethyliaceae and Methanosarcinales will only be resolved with additional research, in which a pure culture is studied to isolate a representative of Methanomethyliaceae.

Overall, we do not intend to rule out the significant contribution of the hydrogenotrophic and acetoclastic methanogenic pathways, as they have been repeatedly observed to be involved in methanogenic hydrocarbon degradation in both enrichment cultures and environmental samples. However, this study expands the current knowledge that, at least in the late-exponential phase, wherein necromass-derived methyl-compounds are available, H_2-dependent methylotrophic methanogenesis and methylotrophic methanogenesis may also play major roles in the conversion of alkanes to methane. H_2-dependent methylotrophic and methylotrophic methanogenesis may have been overlooked in previous enrichment cultures because they were harvested earlier than the late-exponential phase [19,20,23]. Another possible reason for this difference is that the initial inoculums for previous cultures (mostly oil reservoir production waters and ditch sediments) are different from that used in this study (OS from oil refinery) [5,23]. Based on the results of this study, as well as the fact that obligate methylotrophic methanogens (such as *Methanohalophilus* and *Methanolobulus*) and facultative methylotrophic methanogens (such as *Methanosarcina*) are ubiquitous in hydrocarbon-associated environments [21,69], these organisms may be assigned the ecological role of methylotrophic methanogenesis from necromass-derived methyl-compounds.

Herein, we found that the transcripts of several MAGs were below the detection limit, which was unexpected, as some possessed a high relative abundance in the metagenome. Nevertheless, the extremely low transcriptional levels were consistent with the previous descriptions of metatranscriptomes from biodegraded oil fields [18]. A possible reason for this may be the extremely small growth rate of methanogenic alkane-degrading cultures, which implies that very little gene expression occurred. The metagenomic analysis demonstrated that the transcriptionally underrepresented members have a metabolic potential associated with methanogenic alkane degradation and may actively participate in this process at a time before sampling. Note that the results of this metatranscriptomic analysis are only a snapshot of the microbial activity occurring in the late-exponential phase of methane production. In a future study, increased sampling times are required to capture the overall microbial activity profile at different phases, including the lag, early exponential methane production, mid-exponential methane production, late-exponential, and stationary phases. In addition, H_2-dependent methylotrophic methanogenesis during anaerobic alkane degradation requires further verification, probably by another transfer cultivation combined with DNA-SIP labeling technology.

5. Conclusions

This study evaluated the mechanism of microbial methanogenic alkane degradation, revealing that H_2-dependent methylotrophic methanogens, as well as methylotrophic methanogens, may play an important ecological role in the carbon cycle in hydrocarbon-associated environments. Additionally, we achieved sustained improvements in the kinetic properties of methane production in the alkane-degrading consortium through several enrichment cultivations, thereby demonstrating potential remediation of hydrocarbon-contaminated anoxic environments. Overall, this study will help to inform technologies that the microbially enhanced energy recovery of petroleum from marginally productive oil fields may convert approximately 30% of the total crude oil remaining underground as residues into methane gas, which can then be easily recovered.

Acknowledgments

This work was supported by grants of National Natural Science Foundation of China (42061134011, 52074129, and 42173076); the Natural Science Foundation of Shanghai (21ZR1417400); the Shanghai International Collaboration Program (18230743300); the Fundamental Research Funds for the Central Universities (JKJ012016028) to Yi-Fan Liu, Li-Bin Shou, Shi-Zhong Yang, Jin-Feng Liu, and Bo-Zhong Mu; and the NSFC/RGC Joint Research Fund (41161160560) to Ji-Dong Gu.

Authors' contribution

Zhao-Wei Hou and Xiao-Lin Wu provided the samples. Li-Ying Wang, Bo Liang and Jing Chen set up the enrichment cultures.

Jing Chen monitors the methane production during incubation. Zhong-Lin Liu performed the PCR experiments. Dan-Dan Lin and Li-Bin Shou were committed to all the experiments. Yi-Fan Liu performed the statistic and metagenomic and metatranscriptomic analysis. Yi-Fan Liu, Ji-Dong Gu, Lei Zhou, and Bo-Zhong Mu wrote the paper. Bo-Zhong Mu oversaw this project. All authors read and approved the final manuscript.

Compliance with ethics guidelines

Yi-Fan Liu, Jing Chen, Zhong-Lin Liu, Zhao-Wei Hou, Bo Liang, Li-Ying Wang, Lei Zhou, Li-Bin Shou, Dan-Dan Lin, Shi-Zhong Yang, Jin-Feng Liu, Xiao-Lin Wu, Ji-Dong Gu, and Bo-Zhong Mu declare that they have no conflict of interest or financial conflicts to disclose.

Appendix A. Supplementary data

Supplementary data to this article can be found online at https://doi.org/10.1016/j.eng.2021.08.027.

References

[1] Kleinsteuber S, Schleinitz KM, Vogt C. Key players and team play: anaerobic microbial communities in hydrocarbon-contaminated aquifers. Appl Microbiol Biotechnol 2012;94(4):851–73.
[2] Ghattas AK, Fischer F, Wick A, Ternes TA. Anaerobic biodegradation of (emerging) organic contaminants in the aquatic environment. Water Res 2017;116:268–95.
[3] Gieg LM, Kolhatkar RV, McInerney MJ, Tanner RS, Harris SH, Sublette KL, et al. Intrinsic bioremediation of petroleum hydrocarbons in a gas condensate-contaminated aquifer. Environ Sci Technol 1999;33(15):2550–60.
[4] An D, Caffrey SM, Soh J, Agrawal A, Brown D, Budwill K, et al. Metagenomics of hydrocarbon resource environments indicates aerobic taxa and genes to be unexpectedly common. Environ Sci Technol 2013;47(18):10708–17.
[5] Zengler K, Richnow HH, Rosselló-Mora R, Michaelis W, Widdel F. Methane formation from long-chain alkanes by anaerobic microorganisms. Nature 1999;401(6750):266–9.
[6] Mbadinga SM, Wang LY, Zhou L, Liu JF, Gu JD, Mu BZ. Microbial communities involved in anaerobic degradation of alkanes. Int Biodeterior Biodegradation 2011;65(1):1–13.
[7] Gieg LM, Fowler SJ, Berdugo-Clavijo C. Syntrophic biodegradation of hydrocarbon contaminants. Curr Opin Biotechnol 2014;27:21–9.
[8] Siddique T, Penner T, Semple K, Foght JM. Anaerobic biodegradation of longer-chain *n*-alkanes coupled to methane production in oil sands tailings. Environ Sci Technol 2011;45(13):5892–9.
[9] Embree M, Nagarajan H, Movahedi N, Chitsaz H, Zengler K. Single-cell genome and metatranscriptome sequencing reveal metabolic interactions of an alkane-degrading methanogenic community. ISME J 2014;8(4):757–67.
[10] Wawrik B, Marks CR, Davidova IA, McInerney MJ, Pruitt S, Duncan KE, et al. Methanogenic paraffin degradation proceeds via alkane addition to fumarate by '*Smithella*' spp. mediated by a syntrophic coupling with hydrogenotrophic methanogens. Environ Microbiol 2016;18(8):2604–19.
[11] Oberding LK, Gieg LM, Parales RE. Methanogenic paraffin biodegradation: alkylsuccinate synthase gene quantification and dicarboxylic acid production. Appl Environ Microbiol 2018;84(1):e01773-17.
[12] Chen J, Liu YF, Zhou L, Mbadinga SM, Yang T, Zhou J, et al. Methanogenic degradation of branched alkanes in enrichment cultures of production water from a high-temperature petroleum reservoir. Appl Microbiol Biotechnol 2019;103(5):2391–401.
[13] Gieg LM, Duncan KE, Suflita JM. Bioenergy production via microbial conversion of residual oil to natural gas. Appl Environ Microbiol 2008;74(10):3022–9.
[14] Dolfing J, Larter SR, Head IM. Thermodynamic constraints on methanogenic crude oil biodegradation. ISME J 2008;2(4):442–52.
[15] Jones DM, Head IM, Gray ND, Adams JJ, Rowan AK, Aitken CM, et al. Crude-oil biodegradation via methanogenesis in subsurface petroleum reservoirs. Nature 2008;451(7175):176–80.
[16] Cheng L, Ding C, Li Q, He Q, Dai LR, Zhang H, et al. DNA-SIP reveals that Syntrophaceae play an important role in methanogenic hexadecane degradation. PLoS ONE 2013;8(7):e66784.
[17] Embree M, Liu JK, Al-Bassam MM, Zengler K. Networks of energetic and metabolic interactions define dynamics in microbial communities. Proc Natl Acad Sci USA 2015;112(50):15450–5.
[18] Liu YF, Galzerani DD, Mbadinga SM, Zaramela LS, Gu JD, Mu BZ, et al. Metabolic capability and *in situ* activity of microorganisms in an oil reservoir. Microbiome 2018;6(1):5.
[19] Meslé M, Dromart G, Oger P. Microbial methanogenesis in subsurface oil and coal. Res Microbiol 2013;164(9):959–72.
[20] Wang LY, Li W, Mbadinga SM, Liu JF, Gu JD, Mu BZ. Methanogenic microbial community composition of oily sludge and its enrichment amended with alkanes incubated for over 500 days. Geomicrobiol J 2012;29(8):716–26.
[21] Liang B, Wang LY, Mbadinga SM, Liu JF, Yang SZ, Gu JD, et al. Anaerolineaceae and Methanosaeta turned to be the dominant microorganisms in alkanes-dependent methanogenic culture after long-term of incubation. AMB Express 2015;5(1):37.
[22] Wang LY, Gao CX, Mbadinga SM, Zhou L, Liu JF, Gu JD, et al. Characterization of an alkane-degrading methanogenic enrichment culture from production water of an oil reservoir after 274 days of incubation. Int Biodeterior Biodegradation 2011;65(3):444–50.
[23] Liu YF, Chen J, Liu ZL, Shou LB, Lin DD, Zhou L, et al. Anaerobic degradation of paraffins by thermophilic actinobacteria under methanogenic conditions. Environ Sci Technol 2020;54(17):10610–20.
[24] Gu JD. More than simply microbial growth curves. Appl Environ Biotechnol 2017;2(1):63–5.
[25] Symons BGE, Buswell AM. The methane fermentation of carbohydrates. J Am Chem Soc 1933;55(5):2028–36.
[26] Ren G, Zhang H, Lin X, Zhu J, Jia Z. Response of phyllosphere bacterial communities to elevated CO_2 during rice growing season. Appl Microbiol Biotechnol 2014;98(22):9459–71.
[27] Ohene-Adjei S, Teather RM, Ivan M, Forster RJ. Postinoculation protozoan establishment and association patterns of methanogenic archaea in the ovine rumen. Appl Environ Microbiol 2007;73(14):4609–18.
[28] Quast C, Pruesse E, Yilmaz P, Gerken J, Schweer T, Yarza P, et al. The SILVA ribosomal RNA gene database project: improved data processing and web-based tools. Nucleic Acids Res 2013;41(D1):D590–6.
[29] Bankevich A, Nurk S, Antipov D, Gurevich AA, Dvorkin M, Kulikov AS, et al. SPAdes: a new genome assembly algorithm and its applications to single-cell sequencing. J Comput Biol 2012;19(5):455–77.
[30] Langmead B, Salzberg SL. Fast gapped-read alignment with Bowtie 2. Nat Methods 2012;9(4):357–9.
[31] Lan F, Demaree B, Ahmed N, Abate AR. Single-cell genome sequencing at ultra-high-throughput with microfluidic droplet barcoding. Nat Biotechnol 2017;35(7):640–6.
[32] Li H, Handsaker B, Wysoker A, Fennell T, Ruan J, Homer N, et al. the 1000 Genome Project Data Processing Subgroup. The sequence alignment/map format and SAMtools. Bioinformatics 2009;25(16):2078–9.
[33] Wu YW, Simmons BA, Singer SW. MaxBin 2.0: an automated binning algorithm to recover genomes from multiple metagenomic datasets. Bioinformatics 2016;32(4):605–7.
[34] Kang DD, Froula J, Egan R, Wang Z. MetaBAT, an efficient tool for accurately reconstructing single genomes from complex microbial communities. PeerJ 2015;3:e1165.
[35] Alneberg J, Bjarnason BS, de Bruijn I, Schirmer M, Quick J, Ijaz UZ, et al. Binning metagenomic contigs by coverage and composition. Nat Methods 2014;11(11):1144–6.
[36] Sieber CMK, Probst AJ, Sharrar A, Thomas BC, Hess M, Tringe SG, et al. Recovery of genomes from metagenomes via a dereplication, aggregation and scoring strategy. Nat Microbiol 2018;3(7):836–43.
[37] Parks DH, Imelfort M, Skennerton CT, Hugenholtz P, Tyson GW. CheckM: assessing the quality of microbial genomes recovered from isolates, single cells, and metagenomes. Genome Res 2015;25(7):1043–55.
[38] Eren AM, Esen ÖC, Quince C, Vineis JH, Morrison HG, Sogin ML, et al. Anvi'o: an advanced analysis and visualization platform for 'omics data. PeerJ 2015;3:e1319.
[39] Hyatt D, Chen GL, Locascio PF, Land ML, Larimer FW, Hauser LJ. Prodigal: prokaryotic gene recognition and translation initiation site identification. BMC Bioinf 2010;11(1):119.
[40] Kanehisa M, Sato Y, Morishima K. BlastKOALA and GhostKOALA: KEGG tools for functional characterization of genome and metagenome sequences. J Mol Biol 2016;428(4):726–31.
[41] Yin Y, Mao X, Yang J, Chen X, Mao F, Xu Y. dbCAN: a web resource for automated carbohydrate-active enzyme annotation. Nucleic Acids Res 2012;40(W1):W445–51.
[42] Dong X, Greening C, Rattray JE, Chakraborty A, Chuvochina M, Mayumi D, et al. Metabolic potential of uncultured bacteria and archaea associated with petroleum seepage in deep-sea sediments. Nat Commun 2019;10(1):1816.
[43] Eddy SR, Pearson WR. Accelerated profile HMM searches. PLOS Comput Biol 2011;7(10):e1002195.
[44] Søndergaard D, Pedersen CNS, Greening C. HydDB: a web tool for hydrogenase classification and analysis. Sci Rep 2016;6(1):34212.
[45] Aziz RK, Bartels D, Best AA, DeJongh M, Disz T, Edwards RA, et al. The RAST server: rapid annotations using subsystems technology. BMC Genomics 2008;9(1):75.
[46] Menzel P, Ng KL, Krogh A. Fast and sensitive taxonomic classification for metagenomics with Kaiju. Nat Commun 2016;7:11257.
[47] Parks DH, Chuvochina M, Waite DW, Rinke C, Skarshewski A, Chaumeil PA, et al. A standardized bacterial taxonomy based on genome phylogeny substantially revises the tree of life. Nat Biotechnol 2018;36(10):996–1004.
[48] Roberts A, Pachter L. Streaming fragment assignment for real-time analysis of sequencing experiments. Nat Methods 2013;10(1):71–3.
[49] Yamada KD, Tomii K, Katoh K. Application of the MAFFT sequence alignment program to large data-reexamination of the usefulness of chained guide trees. Bioinformatics 2016;32(21):3246–51.

[50] Segata N, Börnigen D, Morgan XC, Huttenhower C. PhyloPhlAn is a new method for improved phylogenetic and taxonomic placement of microbes. Nat Commun 2013;4(1):2304.
[51] Letunic I, Bork P. Interactive Tree of Life (iTOL): an online tool for phylogenetic tree display and annotation. Bioinformatics 2007;23(1):127–8.
[52] Xu D, Zhang K, Li BG, Mbadinga SM, Zhou L, Liu JF, et al. Simulation of *in situ* oil reservoir conditions in a laboratory bioreactor testing for methanogenic conversion of crude oil and analysis of the microbial community. Int Biodeterior Biodegradation 2019;136:24–33.
[53] Callaghan AV. Enzymes involved in the anaerobic oxidation of *n*-alkanes: from methane to long-chain paraffins. Front Microbiol 2013;4:89.
[54] Rabus R, Wilkes H, Behrends A, Armstroff A, Fischer T, Pierik AJ, et al. Anaerobic initial reaction of *n*-alkanes in a denitrifying bacterium: evidence for (1-methylpentyl) succinate as initial product and for involvement of an organic radical in *n*-hexane metabolism. J Bacteriol 2001;183(5):1707–15.
[55] Liu YF, Qi ZZ, Shou LB, Liu JF, Yang SZ, Gu JD, et al. Anaerobic hydrocarbon degradation in candidate phylum 'Atribacteria' (JS1) inferred from genomics. ISME J 2019;13(9):2377–90.
[56] Schouw A, Leiknes Eide T, Stokke R, Pedersen RB, Steen IH, Bødtker G. *Abyssivirga alkaniphila* gen. nov., sp. nov., an alkane-degrading, anaerobic bacterium from a deep-sea hydrothermal vent system, and emended descriptions of *Natranaerovirga pectinivora* and *Natranaerovirga hydrolytica*. Int J Syst Evol Microbiol 2016;66(4):1724–34.
[57] Mardanov AV, Ravin NV, Svetlitchnyi VA, Beletsky AV, Miroshnichenko ML, Bonch-Osmolovskaya EA, et al. Metabolic versatility and indigenous origin of the archaeon *Thermococcus sibiricus*, isolated from a siberian oil reservoir, as revealed by genome analysis. Appl Environ Microbiol 2009;75(13):4580–8.
[58] Khelifi N, Amin Ali O, Roche P, Grossi V, Brochier-Armanet C, Valette O, et al. Anaerobic oxidation of long-chain *n*-alkanes by the hyperthermophilic sulfate-reducing archaeon, *Archaeoglobus fulgidus*. ISME J 2014;8(11):2153–66.
[59] Callaghan AV, Morris BEL, Pereira IAC, McInerney MJ, Austin RN, Groves JT, et al. The genome sequence of *Desulfatibacillum alkenivorans* AK-01: a blueprint for anaerobic alkane oxidation. Environ Microbiol 2012;14(1):101–13.
[60] Lloyd KG, Schreiber L, Petersen DG, Kjeldsen KU, Lever MA, Steen AD, et al. Predominant archaea in marine sediments degrade detrital proteins. Nature 2013;496(7444):215–8.
[61] Ragsdale SW, Pierce E. Acetogenesis and the Wood–Ljungdahl pathway of CO_2 fixation. Biochim Biophys Acta 2008;1784(12):1873–98.
[62] Schuchmann K, Müller V. Autotrophy at the thermodynamic limit of life: a model for energy conservation in acetogenic bacteria. Nat Rev Microbiol 2014;12(12):809–21.
[63] Thauer RK, Kaster AK, Seedorf H, Buckel W, Hedderich R. Methanogenic archaea: ecologically relevant differences in energy conservation. Nat Rev Microbiol 2008;6(8):579–91.
[64] Widdel F, Rabus R. Anaerobic biodegradation of saturated and aromatic hydrocarbons. Curr Opin Biotechnol 2001;12(3):259–76.
[65] Laso-Pérez R, Wegener G, Knittel K, Widdel F, Harding KJ, Krukenberg V, et al. Thermophilic archaea activate butane via alkyl-coenzyme M formation. Nature 2016;539(7629):396–401.
[66] Wang Y, Wegener G, Hou J, Wang F, Xiao X. Expanding anaerobic alkane metabolism in the domain of Archaea. Nat Microbiol 2019;4(4):595–602.
[67] Vanwonterghem I, Evans PN, Parks DH, Jensen PD, Woodcroft BJ, Hugenholtz P, et al. Methylotrophic methanogenesis discovered in the archaeal phylum Verstraetearchaeota. Nat Microbiol 2016;1(12):16170.
[68] Krzmarzick MJ, Taylor DK, Fu X, McCutchan AL. Diversity and niche of archaea in bioremediation. Archaea 2018;2018:1–17.
[69] Li XX, Mbadinga SM, Liu JF, Zhou L, Yang SZ, Gu JD, et al. Microbiota and their affiliation with physiochemical characteristics of different subsurface petroleum reservoirs. Int Biodeterior Biodegradation 2017;120:170–85.
[70] Wang LY, Duan RY, Liu JF, Gu SZ, Yang JD, Mu BZ. Molecular analysis of the microbial community structures in water-flooding petroleum reservoirs with different temperatures. Biogeosciences 2012;9(11):4645–59.
[71] Cheng L, Rui J, Li Q, Zhang H, Lu Y. Enrichment and dynamics of novel syntrophs in a methanogenic hexadecane-degrading culture from a Chinese oilfield. FEMS Microbiol Ecol 2013;83(3):757–66.
[72] Ji JH, Liu YF, Zhou L, Mbadinga SM, Pan P, Chen J, et al. Methanogenic degradation of long *n*-alkanes requires fumarate-dependent activation. Appl Environ Microbiol 2019;85(16):1–10.
[73] Savage KN, Krumholz LR, Gieg LM, Parisi VA, Suflita JM, Allen J, et al. Biodegradation of low-molecular-weight alkanes under mesophilic, sulfate-reducing conditions: metabolic intermediates and community patterns. FEMS Microbiol Ecol 2010;72(3):485–95.
[74] Liang B, Wang LY, Zhou Z, Mbadinga SM, Zhou L, Liu JF, et al. High frequency of *Thermodesulfovibrio* spp. and Anaerolineaceae in association with *Methanoculleus* spp. in a long-term incubation of *n*-alkanes-degrading methanogenic enrichment culture. Front Microbiol 2016;7:1431.
[75] Liu JF, Zhang K, Liang B, Zhou ZC, Yang SZ, Li W, et al. Key players in the methanogenic biodegradation of *n*-hexadecane identified by DNA-stable isotope probing. Int Biodeterior Biodegradation 2019;143:104709.
[76] Neufeld JD, Dumont MG, Vohra J, Murrell JC. Methodological considerations for the use of stable isotope probing in microbial ecology. Microb Ecol 2007;53(3):435–42.
[77] Mbadinga SM, Li KP, Zhou L, Wang LY, Yang SZ, Liu JF, et al. Analysis of alkane-dependent methanogenic community derived from production water of a high-temperature petroleum reservoir. Appl Microbiol Biotechnol 2012;96(2):531–42.
[78] Whitman WB, Bowen TL, Boone DR. The methanogenic bacteria. In: Dworkin M, Falkow S, Rosenberg E, Schleifer KH, Stackebrandt E, editors. The prokaryotes. New York City: Springer New York; 2006. p. 165–207.
[79] Orsi WD. Ecology and evolution of seafloor and subseafloor microbial communities. Nat Rev Microbiol 2018;16:671–83.